2013

Molten Carbonates as an Effective Oxygen Reduction Catalyst for 550–650°C Solid Oxide Fuel Cells

Yunhui Gong

Xue Li
University of South Carolina - Columbia, lixue@cec.sc.edu

Lingling Zhang
University of South Carolina - Columbia, zhang257@cec.sc.edu

Whitney Tharp

Changyong Qin

See next page for additional authors

Publication Info

Published in *Journal of The Electrochemical Society*, Volume 160, Issue 9, 2013, pages F958-F964.

Publisher's Version: http://dx.doi.orgg/10.1149/2.031309jes
Gong, Y., Zhang, L., Tharp, W., Qin, C., & Huang, K. (2013). Molten Carbonates as an Effective Oxygen Reduction Catalyst for 550–650°C Solid Oxide Fuel Cells. Journal of The Electrochemical Society, 160 (9), F958 - F964. http://dx.doi.org/10.1149/2.031309jes

Journal of The Electrochemical Society, **160** (9) F958-F964 (2013)
0013-4651/2013/160(9)/F958/7/$31.00 © The Electrochemical Society

Molten Carbonates as an Effective Oxygen Reduction Catalyst for 550–650°C Solid Oxide Fuel Cells

Yunhui Gong,[a] Xue Li,[a] Lingling Zhang,[a] Whitney Tharp,[a] Changyong Qin,[b] and Kevin Huang[a,*,z]

[a]*Department of Mechanical Engineering, University of South Carolina, Columbia, South Carolina 29201, USA*
[b]*Department of Biology, Chemistry and Environmental Health Science, Benedict College, Columbia, South Carolina 29204, USA*

We report the first study that investigates the use of molten carbonates as an effective catalyst to promote electrochemical oxygen reduction reaction (ORR) at the cathode of intermediate temperature solid oxide fuel cells (IT-SOFCs). A series of binary Li-K carbonate compositions were incorporated into the porous backbones of a commercial cathode assembled in symmetrical impedance cells for electrochemical characterization. Within the temperature range of 550–650°C, we observed that the polarization and ohmic area-specific resistances of the original sample can be significantly reduced by the introduction of molten carbonates. A new ORR charge-transfer model involving two intermediate species CO_5^{2-} and CO_4^{2-} as the fast oxygen absorber and transporter, respectively, was presented as the mechanism for the facile ORR kinetics promoted by molten carbonates.
 [DOI: 10.1149/2.031309jes]

Manuscript submitted April 30, 2013; revised manuscript received June 6, 2013. Published June 18, 2013.

Solid oxide fuel cell (SOFC) offers a great potential to produce electricity, heat and fuels with high efficiency and low emissions.[1] To compete with conventional internal combustion engines (ICEs), the high-efficiency and low-emission SOFC needs to excel in performance and cost. A rational approach for SOFC to achieve that goal is to lower its operating temperature from current 800–1000°C to ≤650°C, such that the overall system cost as well as degradation rate can be reasonably reduced by the use of low-cost materials and increased reliability.[2–5] A challenge to the pursuit of such an intermediate-temperature SOFC (IT-SOFC) is the drastically diminished electrocatalytic activity and increased polarization losses due to the high activation energy of cathode oxygen reduction reaction (ORR).[6–8] To search for highly active IT-cathodes with low activation energy, current research has been primarily focused on the areas of materials development, catalysts nanostructuring and microstructural optimization, which includes, but not limited to (1) exploration of mixed ionic and electronic conducting (MIEC) oxygen-deficient perovskite-structured oxides, e.g. $La_xSr_{1-x}Co_{1-y}Fe_yO_{3-\delta}$ (LSCF),[9] $Sm_xSr_{1-x}CoO_{3-\delta}$ (SSCo),[10] $Ba_xSr_{1-x}Co_{1-y}Fe_yO_{3-\delta}$ (BSCF)[3] and $LnBaCo_2O_{6-\delta}$ (Ln = Pr, Nd, Sm and Gd);[11] (2) introduction of nanostructured ORR-active noble-metal and oxide catalysts into cathode backbones;[12–15] (3) optimization of cathode microstructure to maximize the ORR-active sites.[16–19] However, so far none of the above developments has been successfully employed in commercial SOFCs, and new IT-cathode materials are still in great demand.

Recently, we adopted an unconventional approach in the development of IT-cathodes: use of molten carbonates (MCs) as a catalyst to promote ORR. Previous applications of MC in SOFCs were mainly concentrated on combining MC-phases and solid oxides (e.g., doped CeO_2) to form a composite electrolyte with an enhanced ionic conductivity and suppressed electronic conduction.[20–23] Since MC is also known for its ability to absorb and reduce O_2 at relatively lower overpotential in molten carbonate fuel cells (MCFCs),[24–26] the enhanced performance observed in SOFCs based on MC/solid-oxide hybrid electrolytes could also be attributed to the reduced cathode/electrolyte interfacial polarization by the MC phase. A recent Density Functional Theory (DFT) calculation suggested that the presence of a MC phase in $La_{1-x}Sr_xMnO_{3+\delta}$ (LSM) cathode can stimulate the ORR kinetics by forming two intermediate peroxocarbonates species CO_5^{2-} and CO_4^{2-} through a low-energy oxygen dissociative adsorption process.[27] The existence of CO_4^{2-} as an active and stable species in acidic MC has also been observed by Chen et al with in-situ Raman Spectroscopy.[28]

Here we report that incorporation of MC fine-particles into the porous backbones of a commercial cathode can substantially reduce the polarization resistance of the ORR kinetics at t ≤ 650°C. A new comprehensive electrochemical charge-transfer model is subsequently proposed to understand the fundamentals of the enhanced ORR-kinetics. We elect a commercial MIEC comprised of $La_{0.6}Sr_{0.4}Fe_{0.8}Co_{0.2}O_{3-\delta}$ (LSCF) and $Gd_{0.2}Ce_{0.8}O_{1.9}$ (GDC) as the original cathode for the reason that the ORR-kinetics of this composite cathode is rate-limited by the dissociative adsorption of O_2 at t ≤ 650 °C.[29–31] If the MC can indeed promote the rate of surface oxygen dissociative adsorption, the MC-modified LSCF + GDC cathode will show a lowered polarization resistance.

Experimental

Fabrication of symmetrical impedance cells.— The electrochemical performance of cathodes under investigation was evaluated with a symmetrical impedance cell configuration. The symmetrical impedance cell consisted of a dense LSGM ($La_{0.8}Sr_{0.2}Ga_{0.83}Mg_{0.17}O_{3-\delta}$) electrolyte membrane[32] and two identical thin films of porous LSCF+GDC cathode screen-printed on the two sides of the LSGM electrolyte. The LSGM electrolyte membrane made by tape-casting was approximately 15 mm in diameter and 250 μm in thickness after final sintering.[33]

The ink used to screen-print the two identical layers of porous LSCF+GDC cathode on the LSGM was purchased from a commercial source (Sku: 232202, Fuel Cell Materials). The final tri-layer symmetrical cells were fired at 1100°C for 1 h to achieve a good adhesion of the cathode to the electrolyte. There were no concerns over chemical reactions between LSGM and LSCF at this temperature due to the excellent chemical compatibility between the two perovskite structured materials. The final cathodes were porous and had an effective surface area of 0.75 cm^2 and thickness of 30 μm, respectively. For all electrochemical tests (≤650°C), silver paste (C8829, Heraeus) and silver mesh were used as the current collector.

Synthesis of Li-K carbonates modified and LSCF-infiltrated cathodes.— A series of binary Li-K carbonate compositions were prepared by melting a mixture of lithium carbonate (99%, Alfa Aesar) and potassium carbonate (99%, Alfa Aesar) at 650°C for 2 hours. The resultant melts were then broken into micron-size powders through ball milling, which were subsequently dispersed into ethanol under ultrasonic stirring to yield a suspension. A controlled amount of the suspension was then uniformly spread over the cathode surface using a pipette, followed by drying at 100°C. A final heat-treatment was carried out at 650°C for 2 hours to allow carbonates to melt and incorporate into pores of the cathode backbones. The compositions of the binary Li-K carbonate melts was varied from Li/K = 10/90 to

*Electrochemical Society Active Member.
zE-mail: kevin.huang@sc.edu

70/30 (mol%), including the eutectic composition at 62/38. MC loading on the cathode performance was also investigated as a variable.

A competing method to the MC approach of this study for the enhancement of cathode performance is the conventional solution-infiltration. To compare the effectiveness of the two methods in promoting ORR-kinetics, we also prepared LSCF-infiltrated LSCF+GDC cathode from solutions. The precursor solutions were nitrates with a concentration of 0.5 $mol \cdot L^{-1}$. They were prepared by mixing reagent grade $La(NO_3)_3 \cdot 6H_2O$ (Alfa Aesar), $Sr(NO_3)_2$ (Alfa Aesar), $Co(NO_3)_3 \cdot 6H_2O$ (Alfa Aesar) and $Fe(NO_3)_3 \cdot 6H_2O$ (Alfa Aesar) in a desirable stoichiometry to achieve the final nominal composition of $La_{0.6}Sr_{0.4}Co_{0.2}Fe_{0.8}O_{3-\delta}$. The infiltration process was repeated on LSCF + GDC cathode and vacuum condition for 5 times. After each infiltration, the samples were fired at 500°C for 1 h to decompose nitrates into oxides before the next infiltration. The sample was finally calcined at 800°C for 2 h to form the desirable perovskite phase.

Electrochemical and microstructural characterizations.— The spectra of Electrochemical Impedance Spectroscopy (EIS) was collected from the fabricated symmetrical impedance cells using an electrochemical workstation (IM6, Zahner) under open-circuit conditions, and further analyzed with the Thale equivalent circuit software (Zahner) to extract electrode polarization resistance. The area specific resistance (ASR) was converted from the obtained raw polarization resistances by normalizing it to the actual cathode area (0.75 cm^2). The frequency was swept from 10^5 to 0.01 Hz with 20 mV of stimulus AC amplitude. In order to avoid the interference from silver paste,[33] the highest temperature of all the tests was limited to 650°C. The long-term stability of both original and MC-added cathodes was simultaneously evaluated at 600°C for a total of 1,500 hours with a side-by-side cell arrangement.

The microstructures of cathodes in all the symmetrical impedance cells, either pretested or post-tested, were examined with a field-emission scanning electron microscopy (FESEM, Zeiss Ultra) equipped with an energy dispersive X-ray spectroscopy (EDS) analyzer.

Results

The effect of Li-K carbonate loading on R_P and R_O.— The mass loading effect of MC on area-specific resistance (ASR) of the cathode is shown in Figure 1. For this study, the MC composition was fixed at the eutectic composition of Li/K = 62/38 (mol%). At the first glance of EIS spectra at 600°C in Figure 1a, the total ASR of the pristine cathode is largely dominated by the high polarization ASR (denoted as R_P) defined as the length on the real-axis between the highest- and lowest-frequency intercepts. As carbonate is added into the cathode, substantial reduction in R_p from its original value is observed. A quantified comparison as a function of MC loadings at three temperatures of 550, 600 and 650°C is further illustrated in Figure 1b and 1c. The height of bar represents the percentage of R_P and R_O in relative to those of the pristine sample. It appears that the optimal loading of MC at which the lowest R_p was found is 3.6 $mg \cdot cm^{-2}$. The lowest R_P obtained at 3.6 $mg \cdot cm^{-2}$ represents less than 1% that of the pristine sample within 550–650°C. The degree of R_P-reduction is also noted to be less temperature-sensitive. For a given MC loading, R_P decreases with temperature, exhibiting a typical thermally-activated polarization process. Along with the R_P reduction, MC also led to a decrease in ohmic ASR (R_O) by ~60% over the pristine sample (here R_O is defined as the highest-frequency intercept with the real-axis). Since the measured R_O contains a large contribution from the electrolyte, the extent of MC-effect on R_O could be somewhat diluted. Among the different MC loadings (1.2–4.8 $mg \cdot cm^{-2}$) evaluated, there is a little effect observed on R_O.

The effect of Li-K carbonate composition on R_P and R_O.— The effect of Li-K carbonate composition on R_P and R_O was also investigated, results of which are shown in Figure 2 as the original EIS

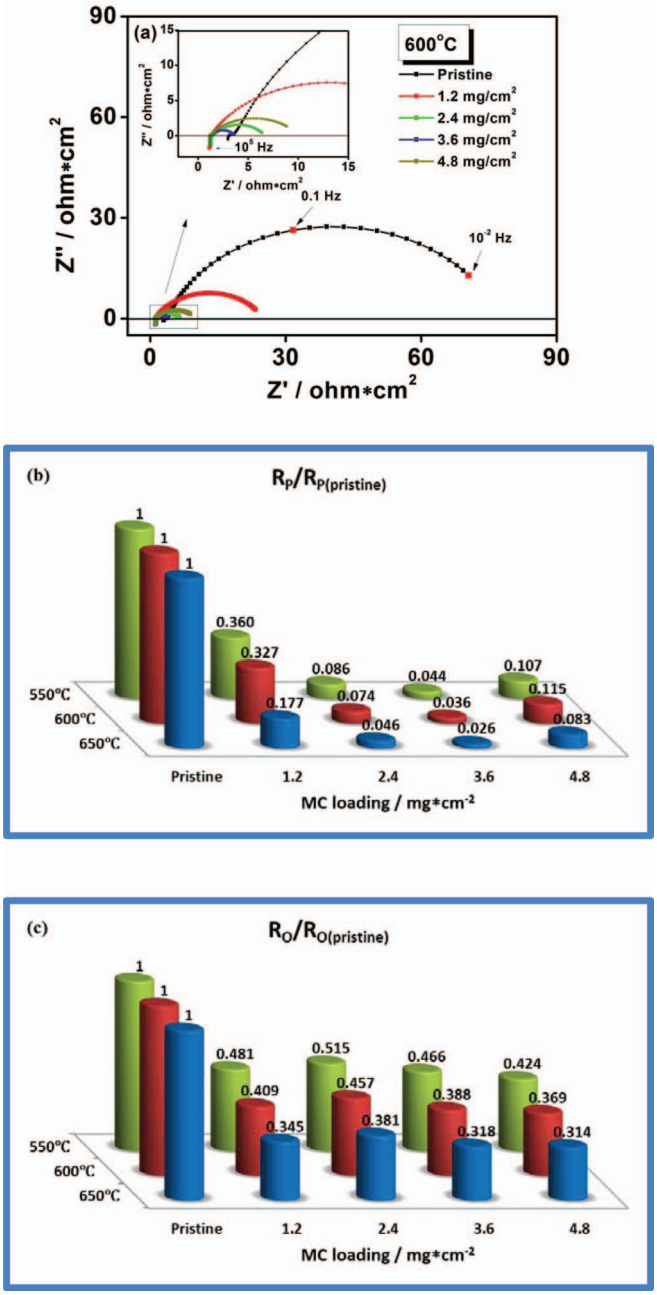

Figure 1. (a) EIS spectra measured from pristine and MC-modified LSCF+GDC cathodes at 600°C; (b) normalized R_P and (c) R_O as a function of MC mass-loading at 550, 600, 650°C.

spectra in Figure 2a, extracted R_P in Figure 2b and R_O in Figure 2c, respectively. For this study, the MC loading is fixed at 3.6 $mg \cdot cm^{-2}$. All of the MC compositions led to reduction in R_P and R_O in compared to the pristine sample. The highest R_P-reduction in Figure 2b is observed on the eutectic composition Li/K = 62/38 (mol%), followed by compositions of Li/K = 30/70, 70/30 and 10/90. Similar to Figure 1c, R_O does not show appreciable variations among compositions of Li/K = 70/30, 30/70 and 62/38, but indeed increase with the composition of Li/K = 10/90.

Comparison of MC-modified and solution-infiltrated LSCF cathodes.— The advantage of MC modification over conventional infiltration method to enhance the performance of cathodes is shown in Figure 3a, where the measured R_P and R_O of MC-modified LSCF+GDC cathode are directly compared with the pristine and

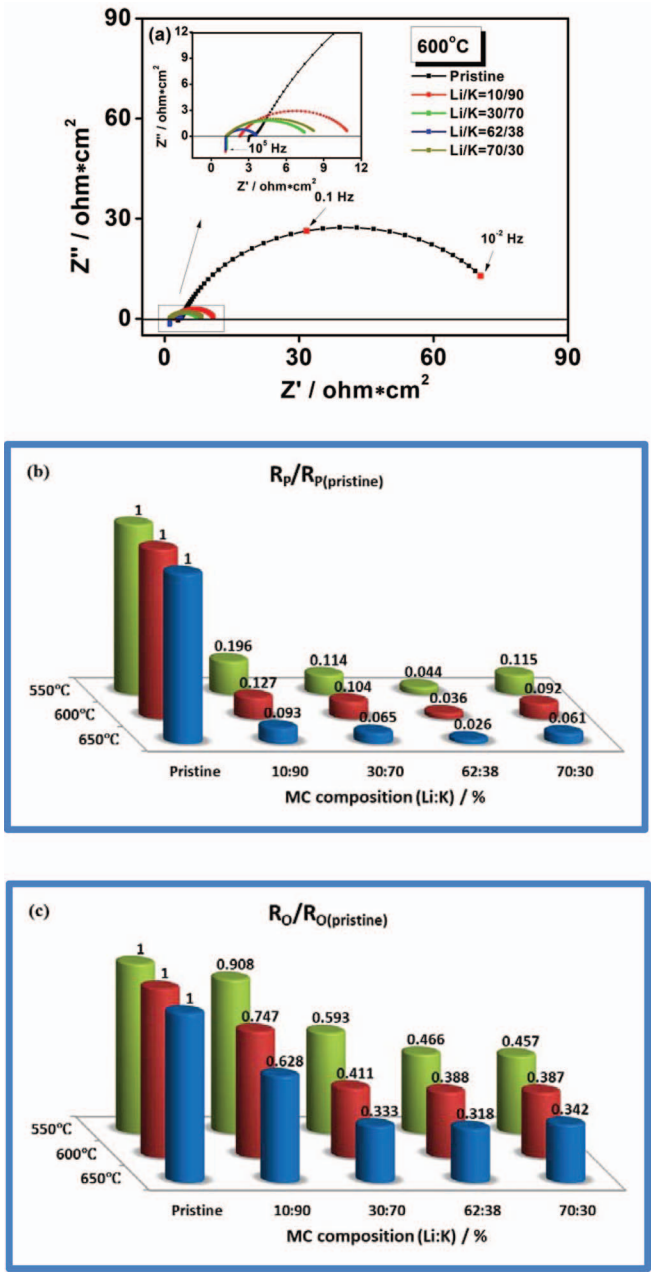

Figure 2. (a) EIS spectra measured at 600°C from pristine cathode and modified LSCF+GDC cathodes with different L-K MC compositions; (b) normalized R_P and (c) R_O as a function of MC composition at 550, 600, 650°C. The MC mass-loading is fixed at 3.6 mg · cm^{-2}.

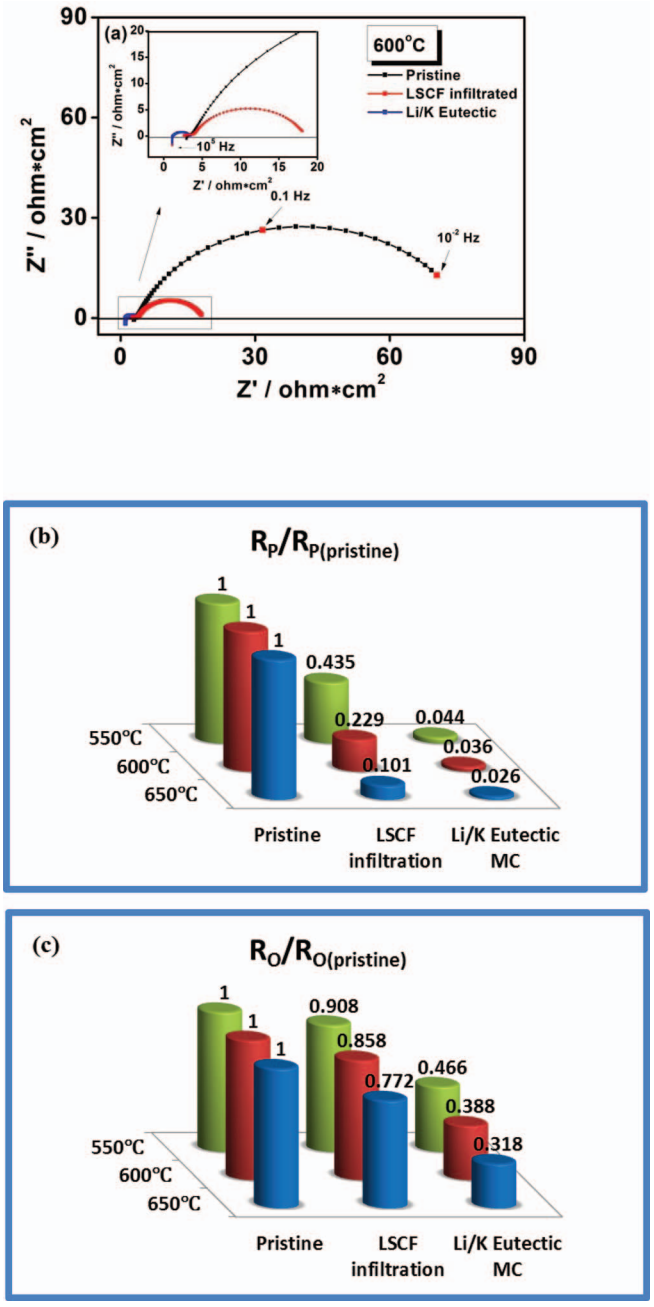

Figure 3. (a) EIS spectra of the pristine, LSCF-infiltrated and MC-modified LSCF+GDC cathodes measured at 600°C; quantified R_P (b) and R_O (c) comparisons at 550, 600 and 650°C.

LSCF-infiltrated counterparts. Although the two modified cathodes exhibit considerable reduction in R_P over the pristine one, the degree of R_P- and R_O-reduction achieved by MC is far superior to that by infiltrated LSCF. Figure 3b summarizes all the R_p and R_O values obtained from three cathodes within 550–650°C. It is clear that the MC is an excellent catalyst for ORR, exhibiting the lowest R_P and R_O.

It should be noted that preparation of MC-modified cathode is a rather easy process. It can be performed by single-step dispersion of a small fraction of MC ethanol suspension into the cathode backbones, followed by a one-time heat-treatment at 650°C. In contrast, the solution-infiltrated LSCF cathode requires a repetitive and tedious process to prepare, making it production unfriendly.

Long-term stability.— Long-term stability of a cathode is an important requirement for SOFCs to be a commercial product. To demonstrate the suitability of MC-modified cathodes for practical long-term uses, the R_P and R_O of the pristine and MC-modified cathodes were constantly monitored at 600°C over 1,500 hours shown in Figure 4. The behavior of the pristine sample can be characterized by an initial decrease in R_p and R_O for the first 300-hour, followed by a gradual increase. Such an early-stage reduction in R_P and R_O is attributed to the well-known "break-in" phenomenon involving interfacial reconfiguration.[34] Since there is no obvious microstructural change found (see later Figure 5), the increases in R_P and R_O of the pristine LSCF cathode are likely attributed to the Sr segregation on the surface of cathode as suggested in the literature.[35] In contrast, the MC-modified cathode shows not only much lowered R_P and R_O but

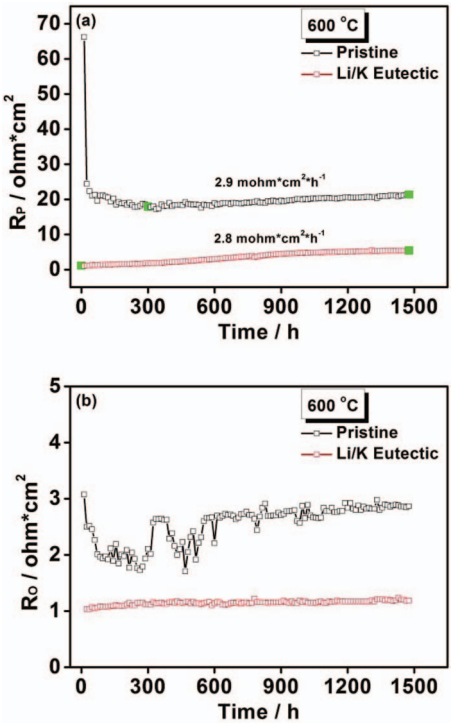

Figure 4. Long term stability of R_P and R_O of pristine and MC-modified LSCF+GDC cathodes evaluated at 600°C; (a) R_P, (b) R_O.

also no "break-in" effect. The absence of the "break-in" effect for the MC-modified cathode implies that the cathode may have been pre-activated by the presence of MC phase during the sample preparation. The similar rate of R_P-increase observed for both samples during the entire testing period seems to suggest a similar degradation mechanism, *i. e.*, Sr-segregation. Furthermore, lower and smoother variation of R_O of the MC-modified sample than the pristine one during the test also suggests that the effective conductivity of the cathode has been enhanced by MC.

Microstructural observations.— To further facilitate the understanding of MC-promoted ORR kinetics, the microstructural features of pristine and MC-modified cathodes before and after 1,500-hours testing were characterized with SEM/EDS. The cross-sectional views of microstructures near the cathode/electrolyte interface of the two samples are shown in Figure 5. The pristine cathode in Figure 5a and 5b shows a typical porous microstructure with connected LSCF and GDC networks. After the 1,500-hours test at 600°C, no obvious difference in microstructure can be discerned. However, for the MC-modified cathode, a clearly distinguishable microstructure is observed in Figure 5c and 5d. For the pre-test sample, randomly distributed needle-like species are seen over the internal surfaces of cathode backbones. Local EDX analysis indicated that these slender needles belong to the Li/K carbonates. The EDX analysis on the post-tested sample (1,500-hours), however, revealed no trace of carbonates on the surfaces of cathode grains. The surface of the MC-modified sample seems uneven in Figure 5d, a sign of MC dissolution into LSCF. Decomposition of carbonates into oxide and CO_2 should not be the cause for the MC disappearance as it has been previously reported in the literature that 0.03% CO_2 in air is sufficient to prevent the decomposition.[36] While the exact chemical change occurred within the cathode during testing is unclear and worth further investigating, it is interesting to note that alkaline-earth and rare-earth elements such as those used in LSCF and GDC have been reported as the enhancers for oxygen solubility in MC.[37]

Single cell performance.— Figure 6 compares the power characteristic of the pristine and MC-modified single SOFCs. Both cells exhibited reasonable OCV, indicating a good sealing. The performance of the pristine cell was very poor, in part due to the use of a thicker LSGM membrane, but mainly due to the poor cathode performance as was also confirmed by the EIS results of half-cell impedance

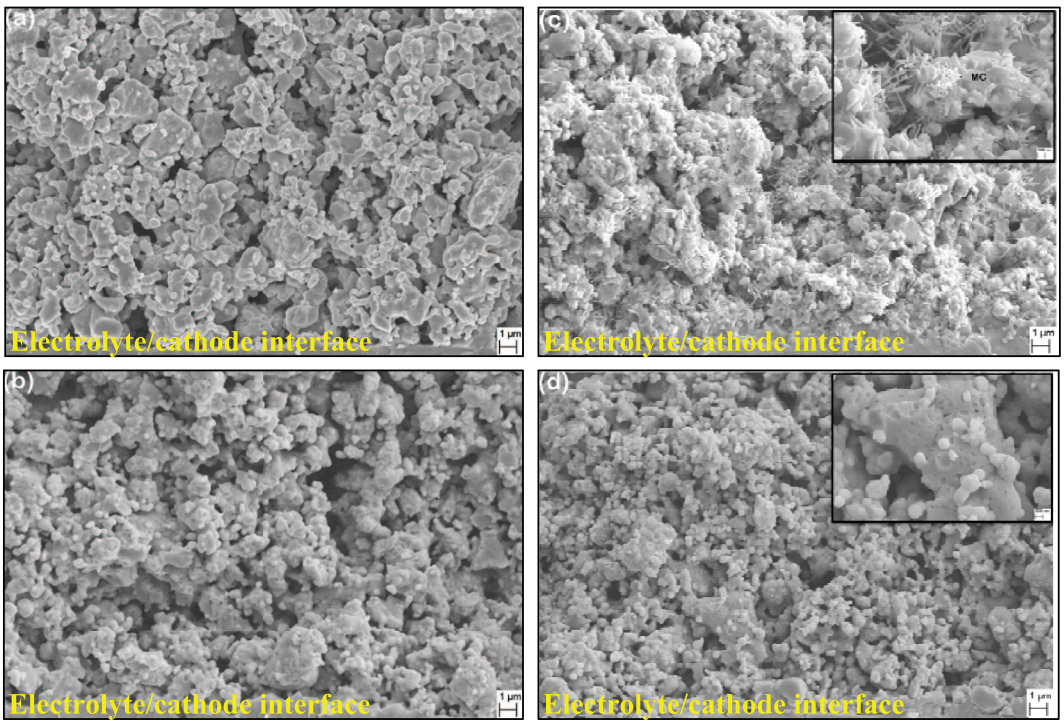

Figure 5. Microstructural changes of the cathodes recorded before and after 1,500-h test at 600°C. Pristine cathode: (a) before and (b) after 1500-h test; MC-modified cathode: (c) before and (d) after 1500-h test.

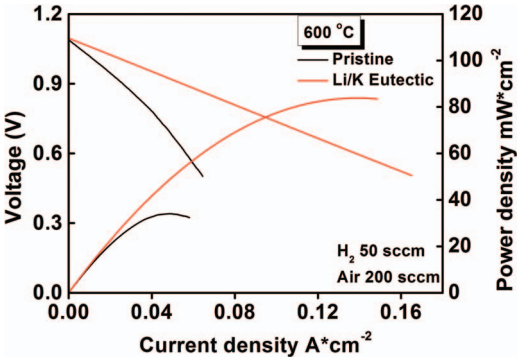

Figure 6. V-I and P-I curves of the pristine and MC-modified single cells at 600°C.

analysis shown in the previous section. A factor of three performance improvement by MC-incorporation in cathode microstructure is seen from Figure 6, although the overall performance was not as high as expected.

Discussion

A new ORR charge-transfer model involving MC phase.— The advantages of MC as an effective ORR-catalyst to reduce R_P and R_O of the pristine LSCF+GDC cathode are clearly demonstrated. To understand how MC involves in and promotes the ORR kinetics, a new charge-transfer model is herein proposed. The model is centered on the hypothesis of two oxygen-rich peroxycarbonate-ions CO_5^{2-} and CO_4^{2-} species as the fast oxygen absorber and transporter, respectively. Figure 7a illustrates schematically the concept of the chemisorption of CO_2 on the surface of MC and subsequent reaction with CO_3^{2-} to form CO_5^{2-} and CO_4^{2-} as the intermediate species, respectively.

The theoretical support to the proposed ORR charge-transfer model is provided by DFT calculations. First, the surface chemisorption of O_2 molecules on MC is a thermodynamically favorable process as indicated by the negative Gibbs free energy at the standard state ($\Delta G^o = -101.6$ kJ/mole) for the reaction of $CO_3^{2-} + O_2 = CO_5^{2-}$. Partial charge-transfer occurred from MC to oxygen during the formation of CO_5^{2-} lowers the energy of stabilization.[27] Second, the equilibrium constant K = 1.1 at 873K for the subsequent reaction of CO_5^{2-} with CO_3^{2-}, i.e., $CO_5^{2-} + CO_3^{2-} = 2CO_4^{2-}$, suggests a good chemical stability of CO_4^{2-} in the bulk of MC. Third, Figure 7b of molecular orbitals and energy eigenvalues calculated by DFT shows that CO_4^{2-} has the lowest reduction potential of oxygen compared to CO_5^{2-} and O_2^{2-}, suggesting CO_4^{2-} as a likely active species to be involved in the charge-transfer step of the ORR.[27] From these preliminary DFT calculations, it is reasonable to assert that CO_5^{2-} and CO_4^{2-} other than O_2^{2-} or O_2^- play an active role in the MC-involved ORR kinetics.

The experimental support to the proposed charge-transfer model is the spectroscopic observation of CO_4^{2-} [28] and the measured high oxygen solubility in MC.[38,39] The strong affinity of O_2 to MC in the form of CO_5^{2-} can lead to a very high sticking coefficient of oxygen molecules onto the surface of MC. On the contrary, classical

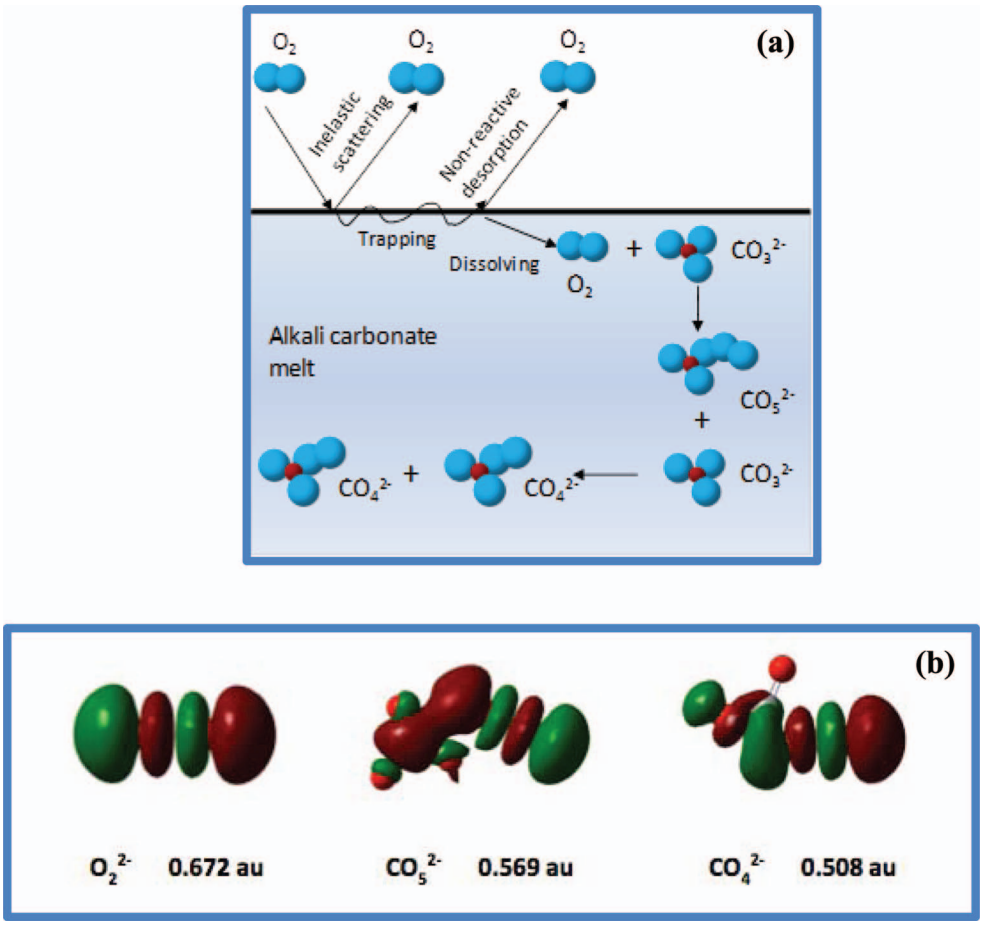

Figure 7. (a) Schematic illustration of how oxygen molecules are chemisorbed by MC and converted into CO_5^{2-} and CO_4^{2-}, respectively; (b) Sigma anti-bonding orbitals of O_2^{2-}, CO_5^{2-} and CO_4^{2-} species modeled by DFT.

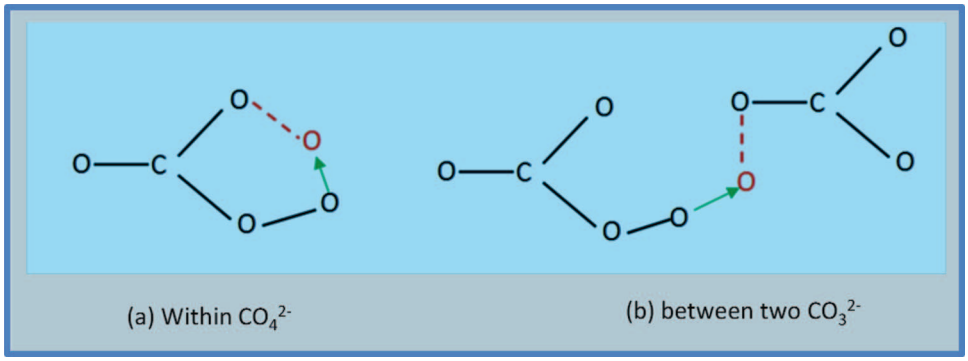

Figure 8. Schematic of the cooperative "cogwheel" mechanism illustrating how oxygen is transported in the form of CO_4^{2-} through MC phase.

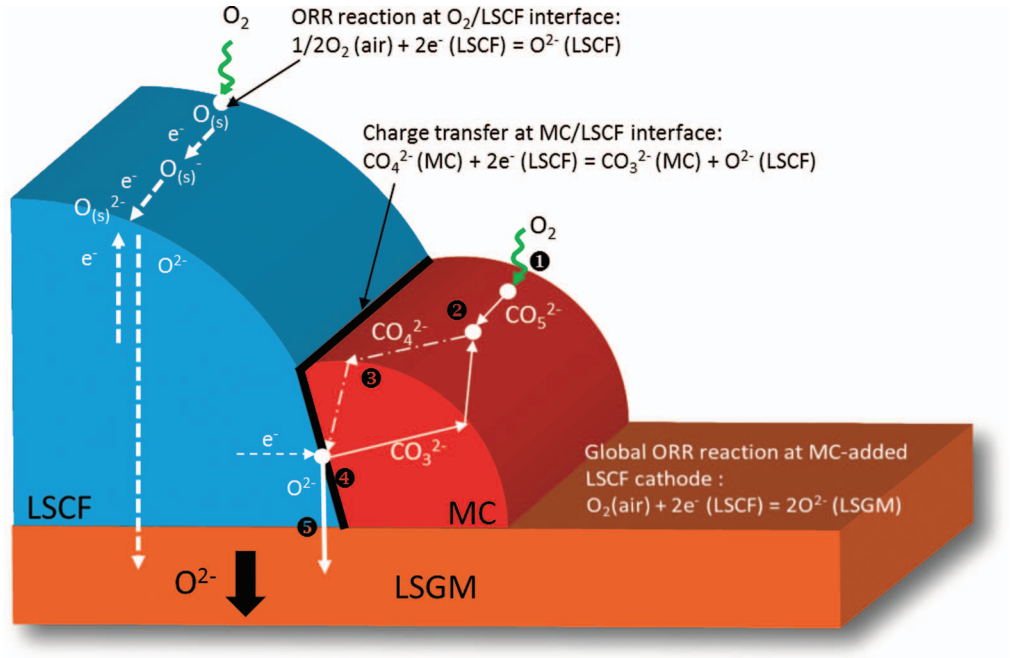

Figure 9. Schematic representation of the new charge-transfer model proposed for MC-promoted ORR. LSGM is used as the model electrolyte.

dissociative chemisorption of gas molecules on ionic solid surfaces typically has a very low sticking coefficient, thus severely limiting the rate of chemisorption.

The migration of CO_4^{2-} from the O_2/MC surface of chemisorption to the MC/LSCF interface of CO_4^{2-} reduction can be achieved through a cooperative "cogwheel" (or "paddle-wheel") mechanism shown in Figure 8, involving the breaking and reforming O–CO_3^{2-} bond. Similar mechanism has also been previously proposed for the superionic conduction phenomenon in fast alkali-metal ionic conductors with rotationally disordered complex anions[40–42] and Ga-based oxides with tetrahedral moieties.[43] The weakly bonded O in CO_4^{2-} (O-CO_3^{2-}) ions can swiftly migrate toward the MC/LSCF interface, where CO_4^{2-} is reduced by electrons from LSCF into O^{2-} and CO_3^{2-}. The O^{2-} ions continue to migrate through LSCF bulk toward the electrolyte, whereas CO_3^{2-} ions return to the MC bulk to replenish the preceding reactions. Again, the electrons transfer is a much faster process at liquid/solid interfaces than at gas/solid interfaces, resulting in facile ORR kinetics. Figure 9 illustrates schematically the five basic steps of the MC-involved ORR, along with the conventional gas/solid charge-transfer pathway, and Table I further summarizes the elementary ORR steps stated above involving CO_5^{2-} and CO_4^{2-} as the intermediate species.

Application of the new ORR charge-transfer model to Figure 2, the observed lowest R_P at the eutectic composition can then be understood as a result of the maximum amount of melt available for catalyzing the ORR. Other compositions are two-phase mixtures according to the phase diagram, containing a portion of solid phase that is inactive to the ORR. On the other hand, finely dispersed MC particles within

Table I. A new charge-transfer model for MC-promoted ORR.

Step-❶: surface oxygen chemisorption at the O_2(air)/MC interface:
$CO_3^{2-}(MC) + O_2(air) = CO_5^{2-}(MC)$
Step-❷: interaction between CO_5^{2-} and CO_3^{2-} in the bulk of MC:
$CO_5^{2-}(MC) + CO_3^{2-}(MC) = 2CO_4^{2-}(MC)$
Step-❸: ionic transport through the MC phase toward MC/LSCF interface:
$CO_4^{2-}(O_2/MC) = CO_4^{2-}(MC/LSCF)$
Step-❹: charge transfer at the MC/LSCF interface:
$CO_4^{2-}(MC) + 2e^-(LSCF) = CO_3^{2-}(MC) + O^{2-}(LSCF)$
Step-❺: oxide-ion transfer across LSCF/LSGM interface:
$O^{2-}(LSCF) = O^{2-}(LSGM)$
Overall ORR at LSCF cathode:
$O_2(air) + 4e^-(LSCF) = 2O^{2-}(LSGM)$

the porous backbones of the cathode are of high preference in terms of maximizing the reactive area and shortening the distance for CO_4^{2-} to migrate. Overloading the MC in the cathode's porous backbones may, therefore, reduce the reactive area and lengthen the migrating distance of CO_4^{2-}, thus causing impedance to charge-transfer. This is why an optimal MC mass-loading is observed in Figure 1.

R_O reduction by MC.— The R_O measured from the symmetrical impedance cells is the sum contributions from electrolyte, cathode, interfacial contacts, current-collector and measuring leads. Since there are nearly no difference in electrolyte, current-collector and electrical contact among cells tested, the observed reduction in R_O by MC must be originated from the cathode itself. However, the relatively low conductivity of MC phase (e.g., 1.1 $S \cdot cm^{-1}$ at 600°C)[44] in comparison to that of LSCF cathode is not sufficient to justify MC as the sole source for the reduced R_O. Formation of more conductive phase and/or removal of insulating phases from the surface of cathode are possible causes. The fact that EDX analysis does not reveal any trace of Li or K on the surface of cathode after the 1,500-hours test seems to suggest that Li and K get dissolved into LSCF grains during the test. While the exact roles of these cations played in the ORR kinetics and ohmic resistance remains an open question, it is interesting to note that alkaline earth and rare earth elements have been reported as the enhancers for oxygen solubility in MC.[37]

The high R_P of the pristine cathode.— It should be noted that the R_P value of the commercial pristine LSCF+GDC cathode employed in this study is noticeably higher than those reported in the literature.[9] One possible source of discrepancy could arise from how the current collector is treated during the electrochemical testing. We have recently argued that silver metal commonly used as a current collector in electrochemical tests become highly mobile and ORR-active at $t > 650°C$.[33] The volatile silver species then transport to the porous backbones of the cathode and promote the ORR kinetics as a catalyst. The involvement of silver in ORR thus exaggerates the true performance of the original cathode under evaluation. In this study, we have limited our testing to $\leq 650°C$ to ensure a true evaluation of MC-modified cathode by minimizing the silver interference. Therefore, the high R_P of the commercial cathode may be a reality. One should also realize that the nature of this study is comparative. The effectiveness of MC in promoting ORR kinetics is best reflected by the relative change of R_P, not necessarily by the absolute values.

Conclusions

In summary, the Li-K MC has been investigated as an effective catalyst for promoting ORR kinetics in IT-SOFCs. The results explicitly show that the incorporation of MC into the porous backbones of a commercial LSCF+GDC cathode can appreciably reduce R_P and R_O of the original cathode. The reduced R_P is only a small fraction of the original cathode within 550–650°C. The optimal composition and loading of the MC phase are found at 62:38 (Li:K in mol%) and 3.6 $mg \cdot cm^{-2}$, respectively. An electrochemical charge-transfer model involving two intermediates species CO_5^{2-} and CO_4^{2-} as the fast oxygen absorber and transporter, respectively, to deliver the oxygen species from gas phase to the cathode/electrolyte interface is proposed to understand the fundamentals of the MC-enhanced ORR-kinetics. The long-term testing shows satisfactory stability over a 1,500-h period. The single cell testing indicates a factor of three improvements in performance by the MC incorporation. Finally, it is worth mentioning that the single-step and cost-effective MC method is a mass-production friendlier process than the conventional solution-infiltration approach as a means of enhancing cathode performance.

Acknowledgment

This work is supported by the U. S. Army Research Laboratory and the U. S. Army Research Office under grant number W911NF-10-R-006.

References

1. B. C. Steele and A. Heinzel, *Nature*, **414**, 345 (2001).
2. R. Doshi, V. L. Richards, J. D. Carter, X. P. Wang, and M. Krumpelt, *J. Electrochem. Soc.*, **146**, 1273 (1999).
3. Z. P. Shao and S. M. Haile, *Nature*, **431**, 170 (2004).
4. H. Huang, M. Nakamura, P. C. Su, R. Fasching, Y. Saito, and F. B. Prinz, *J. Electrochem. Soc.*, **154**, B20 (2007).
5. E. D. Wachsman and K. T. Lee, *Science*, **334**, 935 (2011).
6. J. Fleig and J. Maier, *J. Eur. Ceram. Soc.*, **24**, 1343 (2004).
7. S. B. Adler, *Chem Rev*, **104**, 4791 (2004).
8. F. Tietz, Q. Fu, V. A. C. Haanappel, A. Mai, N. H. Menzler, and S. Uhlenbruck, *Int. J. Appl. Ceram. Technol.*, **4**, 436 (2007).
9. E. P. Murray, M. J. Sever, and S. A. Barnett, *Solid State Ionics*, **148**, 27 (2002).
10. C. R. Xia, W. Rauch, F. L. Chen, and M. L. Liu, *Solid State Ionics*, **149**, 11 (2002).
11. W. Zhou, J. Sunarso, Z. G. Chen, L. Ge, J. Motuzas, J. Zou, G. X. Wang, A. Julbe, and Z. H. Zhu, *Energy Environ. Sci.*, **4**, 872 (2011).
12. S. R. Wang, T. Kato, S. Nagata, T. Honda, T. Kaneko, N. Iwashita, and M. Dokiya, *Solid State Ionics*, **146**, 203 (2002).
13. M. Camaratta and E. Wachsman, *Solid State Ionics*, **178**, 1242 (2007).
14. Y. Sakito, A. Hirano, N. Imanishi, Y. Takeda, O. Yamamoto, and Y. Liu, *J. Power Sources*, **182**, 476 (2008).
15. J. M. Vohs and R. J. Gorte, *Adv. Mater.*, **21**, 943 (2009).
16. M. G. Bellino, J. G. Sacanell, D. G. Lamas, A. G. Leyva, and N. E. Walsoe de Reca, *J. Am. Chem. Soc.*, **129**, 3066 (2007).
17. L. Dieterle, P. Bockstaller, D. Gerthsen, J. Hayd, E. Ivers-Tiffee, and U. Guntow, *Adv. Energy. Mater.*, **1**, 249 (2011).
18. M. E. Lynch, L. Yang, W. T. Qin, J. J. Choi, M. F. Liu, K. Blinn, and M. L. Liu, *Energy Environ. Sci.*, **4**, 2249 (2011).
19. M. J. Zhi, S. Lee, N. Miller, N. H. Menzler, and N. Q. Wu, *Energy Environ. Sci.*, **5**, 7066 (2012).
20. G. Y. Meng, Q. X. Fu, S. W. Zha, C. R. Xia, X. Q. Liu, and D. K. Peng, *Solid State Ionics*, **148**, 533 (2002).
21. B. Zhu, X. T. Yang, J. Xu, Z. G. Zhu, S. J. Ji, M. T. Sun, and J. C. Sun, *J. Power Sources*, **118**, 47 (2003).
22. J. B. Huang, L. Z. Yang, R. F. Gao, Z. Q. Mao, and C. Wang, *Electrochem. Commun.*, **8**, 785 (2006).
23. C. Xia, L. Li, Y. Tian, Q. H. Liu, Y. C. Zhao, L. J. Jia, and Y. D. Li, *J. Power Sources*, **188**, 156 (2009).
24. A. J. Appleby and S. B. Nicholson, *J. Electroanal. Chem.*, **112**, 71 (1980).
25. C. Y. Yuh and J. R. Selman, *J. Electrochem. Soc.*, **138**, 3642 (1991).
26. X. Li, N. S. Xu, L. L. Zhang, and K. Huang, *Electrochem. Commun.*, **13**, 694 (2011).
27. C. Y. Qin and A. Gladney, *Comput. Theor. Chem.*, **999**, 179 (2012).
28. L. J. Chen, C. J. Lin, J. Zuo, L. C. Song, and C. M. Huang, *J. Phys. Chem. B.*, **108**, 7553 (2004).
29. J. A. Lane, S. J. Benson, D. Waller, and J. A. Kilner, *Solid State Ionics*, **121**, 201 (1999).
30. C. C. Kan, H. H. Kan, F. M. Van Assche, E. N. Armstrong, and E. D. Wachsman, *J. Electrochem. Soc.*, **155**, B985 (2008).
31. Y. M. Choi, M. C. Lin, and M. L. Liu, *J. Power Sources*, **195**, 1441 (2010).
32. K. Q. Huang, R. S. Tichy, and J. B. Goodenough, *J. Am. Ceram. Soc.*, **81**, 2565 (1998).
33. Y. H. Gong, C. Y. Qin, and K. Huang, *ECS Electrochem. Lett.*, **2** F4 (2013).
34. M. Shah, P. W. Voorhees, and S. A. Barnett, *Solid State Ionics*, **187**, 64 (2011).
35. S. P. Simner, M. D. Anderson, M. H. Engelhard, and J. W. Stevenson, *Electrochem. Solid State Lett.*, **9**, A478 (2006).
36. I. Trachtenberg and D. F. Cole, in *Fuel Cell Systems-II*, B. S. Baker Editor, p. 269, American Chemical Society, Chicago (1969).
37. M. Schenke, G. H. J. Broers, and J. A. Ketelaar, *J. Electrochem. Soc.*, **113**, 404 (1966).
38. P. L. Spedding and R. Mills, *J. Electrochem. Soc.*, **112**, 594 (1965).
39. A. J. Appleby and C. Vandrunen, *J. Electrochem. Soc.*, **127**, 1655 (1980).
40. M. Jansen, *Angew. Chem.-Int. Edit. Engl.*, **30**, 1547 (1991).
41. S. Shin, Y. Tezuka, A. Sugawara, and M. Ishigame, *Phys. Rev. B*, **44**, 11724 (1991).
42. N. Bagdassarov, H. C. Freiheit, and A. Putnis, *Solid State Ionics*, **143**, 285 (2001).
43. E. Kendrick, J. Kendrick, K. S. Knight, M. S. Islam, and P. R. Slater, *Nat. Mater.*, **6**, 871 (2007).
44. T. Kojima, Y. Miyazaki, K. Nomura, and K. Tanimoto, *J. Electrochem. Soc.*, **154**, F222 (2007).